Available online at www.sciencedirect.com
SCIENCE DIRECT®
Estuarine, Coastal and Shelf Science 68 (2006) 93–100
ESTUARINE COASTAL AND SHELF SCIENCE
www.elsevier.com/locate/ecss

A numerical simulation of the two- and three-dimensional Lagrangian circulation in the northern Gulf of California

S.G. Marinone

Department of Physical Oceanography, CICESE, km 107, Carretera Tijuana-Ensenada, 22800 Ensenada, B.C., Mexico

Received 23 September 2005; accepted 12 January 2006
Available online 31 March 2006

Abstract

The surface circulation in the northern Gulf of California is dominated by a cyclonic gyre during summer and an anticyclonic gyre during winter. The associated 3D Lagrangian circulation is calculated and compared with that detected by surface floats by inhibiting vertical advection in a three-dimensional (3D) numerical model. In general, the 3D circulation follows the same horizontal paths as in the two-dimensional (2D) case but with vertical excursions along the trajectories. However, in some areas, especially those close to the coasts which represents ~20% of the study area, the vertical displacements cause the paths of both cases (with and without vertical advection) to differ considerably, thus resulting in different destinations for the particles. This finding is of relevance for the fate of larvae or contaminants in the area, which so far had been studied on the basis of 2D results alone.

Keywords: gyres; Lagrangian circulation; Gulf of California

1. Introduction

The surface Lagrangian circulation in the northern Gulf of California (Fig. 1) has been described as consisting mostly of a seasonally-reversing gyre, which is cyclonic during summer and anticyclonic during winter (Lavín et al., 1997; Carrillo-Bribiezca et al., 2002). The cyclonic period lasts from June to September, and the anticyclonic period lasts from November to March. These gyres are caused by annual-period forcing by the monsoonal winds, the Pacific Ocean, and the heat flux through the surface (Beier and Ripa, 1999). Summer heating in the northern gulf induces a strong stratification and a dome-like structure of the isopycnals results, favoring the cyclonic circulation. During winter the isopycnals have a concave shape, with a dome structure in dynamic height, thus favoring the anticyclonic circulation (Carrillo-Bribiezca et al., 2002).

The circulation just described has been modeled numerically, from an Eulerian perspective, by Beier (1997) and Palacios-Hernández et al. (2002) with a two-layer model and by Carbajal (1993) and Marinone (2003) with a full three-dimensional (3D) model. The first Lagrangian calculation study of the Gulf of California (Velasco-Fuentes and Marinone, 1999) used a vertically-integrated model to reproduce the horizontal circulation. Gutiérrez et al. (2004) later determined the Lagrangian circulation from the output of Marinone (2003) using only the upper-layer model currents without vertical excursion of the particles and got results in agreement with the surface drifter observations of Lavín et al. (1997).

The purpose of this note is to calculate the 3D Lagrangian trajectories in the northern Gulf of California, using the full 3D current-velocity field of Marinone (2003), and compare the results against those calculations obtained when vertical advection is ignored. Particles are initially released at the surface and tracked for the time period of the winter and summer gyres.

This kind of fixed-depth or depth-averaged horizontal circulation is often used to interpret or derive ideas about properties that are advected by ocean currents (for example, passive pollutants and active larvae). Nevertheless, the real path that water parcels follow in the ocean, where areas of

E-mail address: marinone@cicese.mx

0272-7714/$ - see front matter © 2006 Elsevier Ltd. All rights reserved.
doi:10.1016/j.ecss.2006.01.012

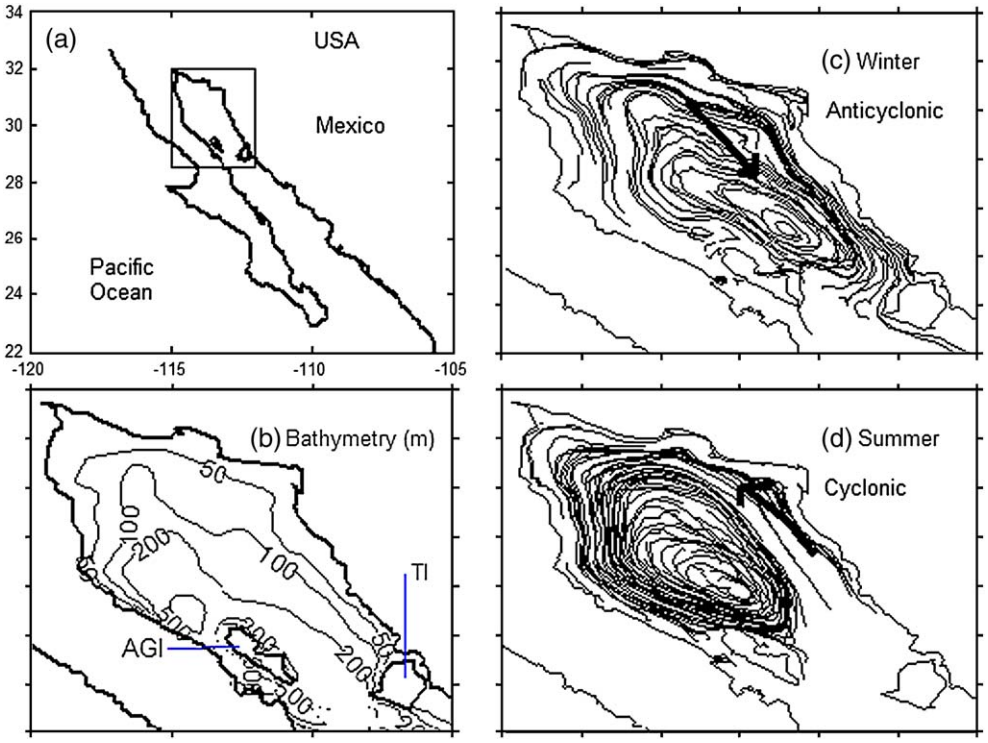

Fig. 1. (a) Study area (rectangle) in the Gulf of California, and (b) bathymetry in meters; AGI and TI stand for Angel de la Guarda and Tiburon Islands, respectively. (c) and (d) show the winter-anticyclonic and summer-cyclonic circulations in the northern gulf. The trajectories are 30 days long and only one particle every 25 (out of 2097) are shown to avoid overcrowding. The large arrows in (c, d) are visual aids to indicate the flow direction.

divergence/convergence occur due to wind and tidal mixing, is expected to differ from the fixed-depth scenario, depending on whether there are, or not, important local vertical velocities. For example, the northern Gulf of California is the site of an important shrimp fishery and during the summer Aragón-Noriega and Calderón-Aguilera (2001) consistently found younger postlarvae off the peninsula coast than off the mainland (mean age of 22 against 28 days old, respectively). This situation is not unexpected, because the general circulation is cyclonic during this period and the reproductive areas have been reported mainly close to the mainland coast, therefore younger postlarvae should be driven toward the mainland first and then towards the peninsular side (older postlarvae downstream). However, Lagrangian studies based on surface circulation alone (for example, Calderón-Aguilera et al., 2003; Marinone et al., 2004) have failed to provide a satisfactory explanation for the observed larvae distribution.

2. Numerical model

Particle trajectories were obtained by time-integrating the velocity field from the layerwise vertically-integrated Hamburg Shelf Ocean Model (HAMSOM) developed by Backhaus (1985). The model is described in detail for the Gulf of California by Marinone (2003), and references therein, focusing on the mean and seasonal global residual circulation. The model domain has a mesh size of $2.5' \times 2.5'$ ($\sim 3.9 \times 4.6$ km) in the horizontal and 12 layers in the vertical with nominal lower levels at 10, 20, 30, 60, 100, 150, 200, 250, 350, 600, 1000 and 4000 m. The model equations are solved semi-implicitly with fully prognostic temperature and salinity fields, thus allowing time-dependent baroclinic motions.

The model is started from rest with a time step of 300 s and is forced with tides, climatological winds, climatological hydrography at the mouth of the gulf, and climatological heat and fresh water fluxes at the air–sea interface. It becomes periodically stable after three years and the results for this note were obtained from the fourth year of the model. As shown by Marinone (2003), the model adequately reproduces the main seasonal signals of surface temperature, heat balance, tidal elevation and surface circulation in the northern Gulf of California as reported by Lavín et al. (1997).

The trajectories of the particles were calculated following the scheme given by Proehl et al. (2005) (see also Visser, 1997; Ross and Sharples, 2004) who state that the Lagrangian trajectories are due to the Eulerian velocity field and a random walk contribution related to eddy diffusivity. The diffusivities are taken from the numerical model, and since the vertical diffusivity is not constant, a pseudo-advective term is introduced to avoid particles to walk away from areas of high to low diffusivities. Therefore, the position of the particles are calculated as:

$$X(t+\delta t) = X(t) + X_a(t) + R_x\sqrt{2A_h\delta t/\sigma_x^2}, \quad (1)$$

$$Y(t+\delta t) = Y(t) + Y_a(t) + R_y\sqrt{2A_h\delta t/\sigma_y^2}, \quad (2)$$

$$Z(t+\delta t) = Z(t) + Z_a(t) + R_z\sqrt{2A_v\delta t/\sigma_z^2} + \delta t\partial A_v/\partial Z, \qquad (3)$$

where (X, Y, Z) are the particle positions in the zonal, meridional, and vertical directions, respectively, at time t, (X_a, Y_a, Z_a) are the advective displacements obtained by integrating the velocity field, $V_a = (u, v, w)$. The velocity at each particle position is calculated by bilinear interpolation of the instantaneous Eulerian velocity fields from the numerical model. R_x, R_y, and R_z are uniform random variables with zero mean and variance σ_x^2, σ_y^2, and σ_z^2, respectively, and vary between -1 and 1. A_h and A_v are the horizontal and vertical diffusivities, respectively. There are no values reported for A_h and A_v in the Gulf of California, therefore the same values of the Eulerian numerical model were used. Eqs. (1) and (2) differ from Eq. (3) in one term, the last in Eq. (3), which takes into account the time and spatial variability of A_v. The horizontal eddy diffusivity is constant ($A_h = 100\ m^2\ s^{-1}$) and therefore the corresponding terms do not contribute to the particle displacements, however, for the vertical, $A_v = A_v(x, y, z, t)$ and the gradient is calculated and interpolated for the individual particle positions each time step. In the numerical model A_v is calculated following Kochergin (1987), as $\alpha\left|\partial/\partial z\, v\right|/(1+\beta Ri)$, where Ri is the Richardson number, $\alpha = 10\ m^2$ and $\beta = 10$. The values of A_v vary from 0 to $\sim 0.03\ m^2\ s^{-1}$ with a temporal and spatial average of $0.013\ m^2\ s^{-1}$ and a standard deviation one order of magnitude smaller.

To test the dependence of the values of A_h in our calculations, we alter them in the last term in Eqs. (1) and (2) from 10 to 200%, (i.e., multiplying them by 0.1 or 10) and found that the general pattern of results does not change. A similar test was performed by Thorpe et al. (2004).

Finally, the trajectories were low-pass filtered to simplify their description. The filter passes about 50% of the amplitude at 0.3 cycles day^{-1} and 95% of the amplitude at 0.08 cycles day^{-1}, while it reduces to less than 1% the diurnal and semi-diurnal amplitudes (Yao et al., 1982). The tidal excursions are small ($\sim$4 km), and if the unfiltered trajectories were retained they would show small elliptic perturbations following the mean path of the particles.

3. Results and discussion

Most of the results shown are restricted to one-month trajectories centered on the times when the gyres are strongest and best defined. One month was also chosen because some fisheries in the northern gulf (e.g. shrimp) last about 2–4 weeks, from the time of spawning to the time that the postlarvae reach the nursery areas (Calderón-Aguilera et al., 2003). Fig. 1c, d shows the 30-day trajectories for winter and summer, respectively, obtained by integrating particles released in the upper layer of the model with zero vertical velocity; this reproduces the numerical results of Gutiérrez et al. (2004), and the observations of Lavín et al. (1997). This agreement with Lavín et al. (1997) is taken as the test of our advective scheme. A 2D plot (x–y plane) of the particle trajectories including vertical advection (not shown) does not visually demonstrate appreciable differences; however, the 3D trajectories (Fig. 2a, b) are notably different. Most of the particles follow the same horizontal path as in the 2D case; that is, they track a cyclonic or anticyclonic gyre depending on the season, but with considerable vertical excursions (Fig. 2c, d) in both seasons.

As shown in Fig. 2, the particles travel up and down during their journey; often the currents at different depths of the water column flow in directions different from those of the surface current. In such cases, a 3D water-parcel trajectory will differ substantially from that of a surface float.

A close inspection of all trajectories shows that the separation between the 2D and 3D paths occurs, in the majority of the cases, when the particles are close to the coast (released there or approach there). To emphasize the cases in which particles travel in different directions depending on whether vertical advection is allowed or not, Fig. 3 shows the trajectories of selected particle releases during winter and summer; the left panels show the 3D paths and the right panels show their horizontal projection. Red lines correspond to the 2D case, and blue and black lines correspond to respective releases for the full 3D case. In the coastal zones and between Tiburon and Angel de la Guarda Islands the paths differ considerably during both summer and winter. During summer the horizontal tracks differ even more when they reach the extreme upper gulf. In the 2D case, some particles stagnate (not shown), whereas their 3D equivalents show vertical displacements due to a convergence of the flow.

How different are, in general, the 2D and 3D trajectories in the northern gulf? To answer this question, the final horizontal distance after a one-month journey for both winter and summer between two particles, one with and the other without vertical advection, released at each grid point was calculated (Fig. 4a, b). Note that the results are assigned to the initial position.

Along the mainland coast, the continental shelf is wider (Fig. 1b) and the currents are stronger there, and thus produce a broader band of differences than off the peninsula side. The larger differences in the final position are found close to the coasts; in the mainland side for winter, and in the peninsular side for summer, while in the northern part of Angel de la Guarda Island the difference is always large. In the central part of the northern gulf the two cases tends to maintain horizontally close. Fig. 4a, c shows the time to escape 50 km from the release point (just for the 3D case, the 2D is very similar but with smaller times and is not shown); near to the center of the gyres and along the peninsular coast the particles remains for two months or more. In the main part of the gyres (see Fig. 1), where the currents are stronger, the particles escape 50 km in just 10–20 days. Many particles (a significant part of the area of Fig. 4a, b) do separates 40 km or more, a distance that may be crucial, for example, for old postlarvae that are trying to reach a nursery area; 40 km away can leave them in a ‘desert’ or low-productivity area.

Fig. 5 gives information about the vertical excursion of the particles for both winter and summer. Fig. 5a, b shows histograms of the mean depths in one month of tracking of

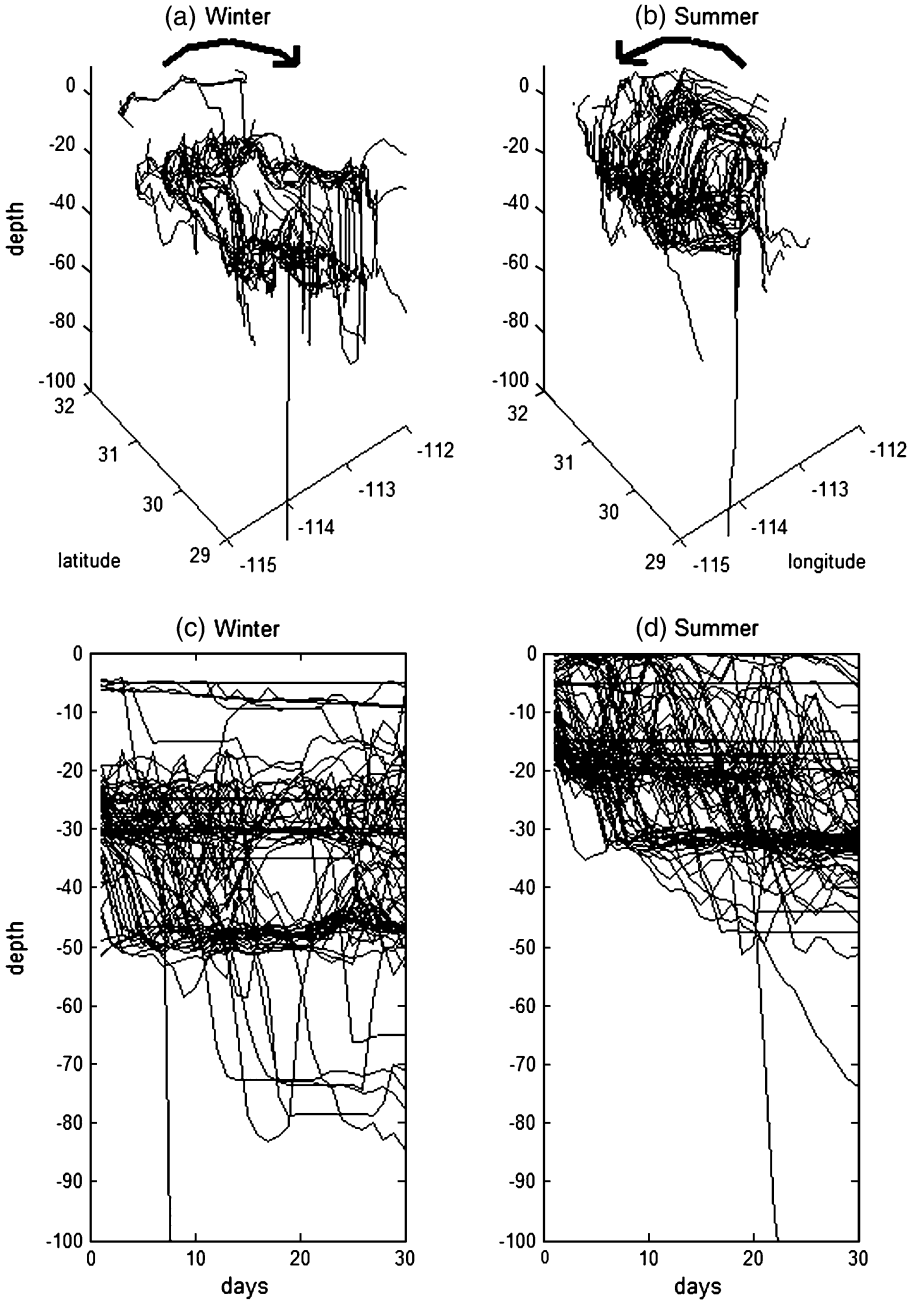

Fig. 2. 3D particle trajectories and time series of their vertical displacement (in meters) for (a, c) winter and (b, d) summer, respectively. The large arrow in (a) and (b) are visual aids for the flow direction. Only one particle every 25 (out of 2097) are shown to avoid overcrowding.

the particles. On average, most of the particles leave the first model layer where they were seeded; during winter, of the 2097 particles 88% have a mean travel depth between 15 and 45 m, while for summer 81% have a mean depth between 5 and 25 m. The difference of the maximum and minimum vertical position (Fig. 5c, d), in one-month journey, results in more particles with smaller difference for winter than for summer; during summer 40% have a difference of ~20 m while 39% have a difference of 30 m in winter. These mean and maximum differences in the vertical excursion of the particles are smaller than the average depth of the area, which is ~130 m. The largest vertical displacements occur in the deep basins and near the sills. At larger depths (not shown), the effect of topography is greater and the particles tend to be trapped following the bathymetry; in many cases, the particles in the 2D case become trapped in a basin, whereas those in the 3D case can escape by traveling up in the water column and then advected out by the shallower flow.

To summarize the results of the difference in horizontal position of the 2D and 3D cases, Fig. 6 shows a time series of the mean difference of all particles during summer and winter, as well as the mean + one standard deviation. As can be seen in the figure, as time passes the final destination keeps

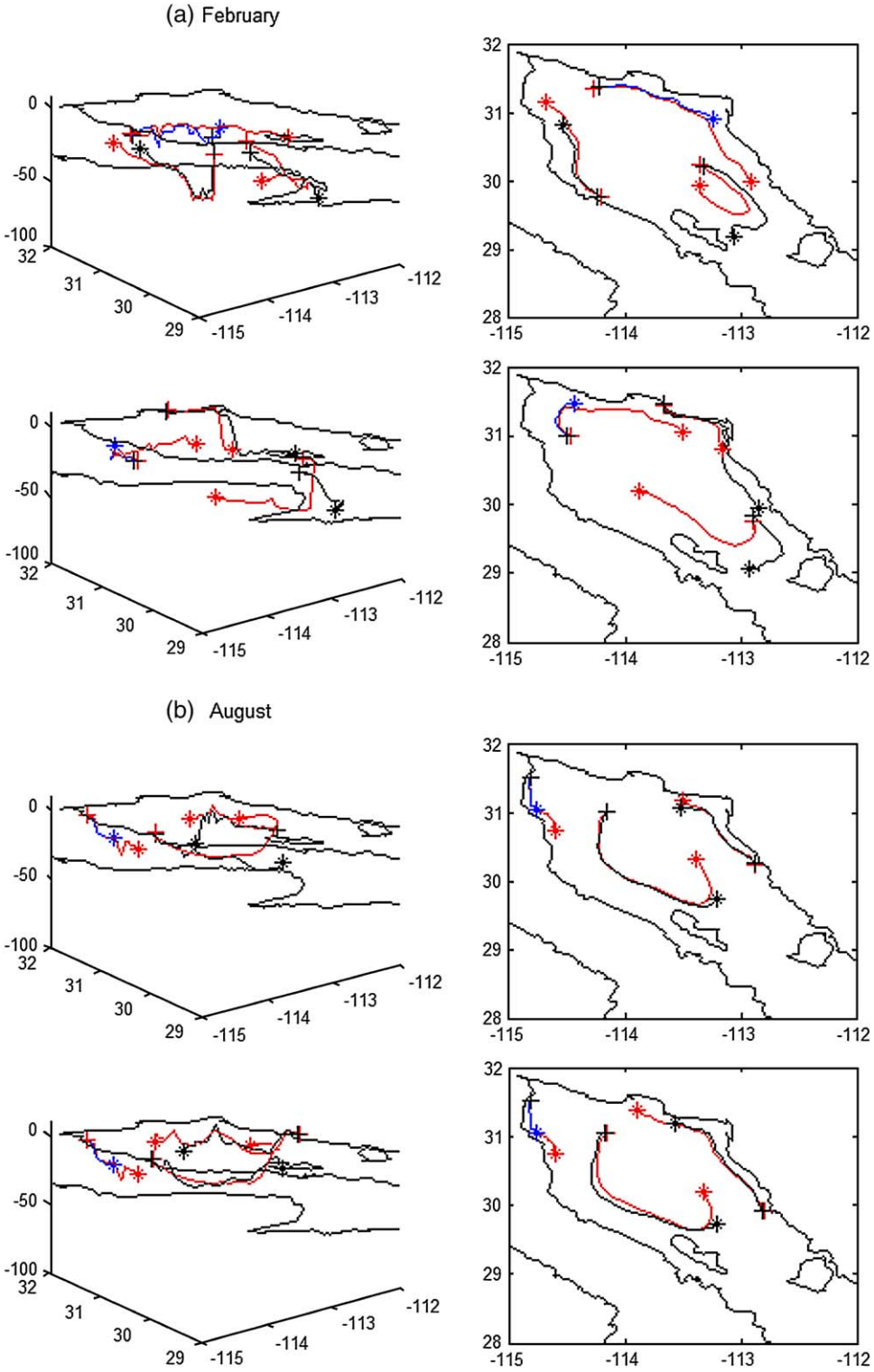

Fig. 3. 3D and 2D trajectories of selected particles during the (a) anticyclonic and (b) cyclonic gyre periods, respectively. Red lines show the paths followed by particles without vertical advection, and blue and black lines show the paths followed by particles with vertical advection included. The initial and final position of the trajectories are marked with a + and *, respectively.

increasing, but in one-month period, the difference in mean position (with a large variability) is ∼31 and 73 km for summer and winter, respectively. As mentioned before, the major departures are close to the coast.

4. Conclusion

In general, the horizontal circulations in the northern Gulf of California for the 2D and 3D cases are very similar.

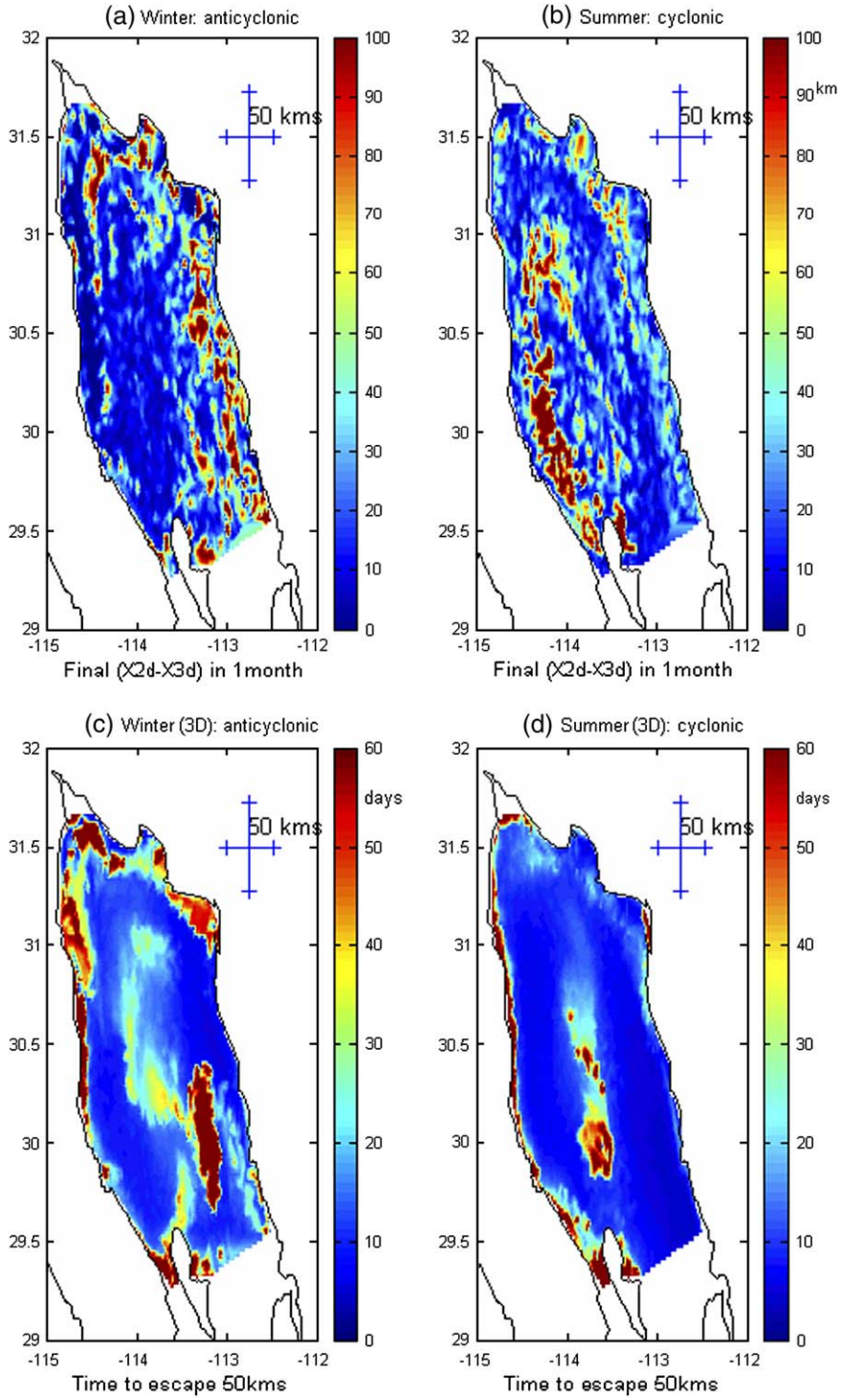

Fig. 4. Distance (km) between two particles released at each grid point, one with and one without vertical advection, after one month, for the (a) anticyclonic and (b) cyclonic gyre periods. Time to escape 50 km radius from the initial position, for the 3D case, for the anticyclonic (c) and cyclonic (d) gyre periods.

However, some particles that undergo large vertical excursions are exposed to differing currents, so that their destination can be very different to that of the 2D case. The areas where most of the large differences where found are close to the coast, accounting for ∼20% of the area (particles) of the northern gulf; in these areas, final destinations can be as far as 40 km apart. Since important nursery areas of shrimp have been reported along the coast, in order to understand why there are older postlarvae upstream instead of downstream, any physical/biological studies of this fishery should require the use of a 3D model of the circulation. The difference in distance obtained from a 2D or 3D in

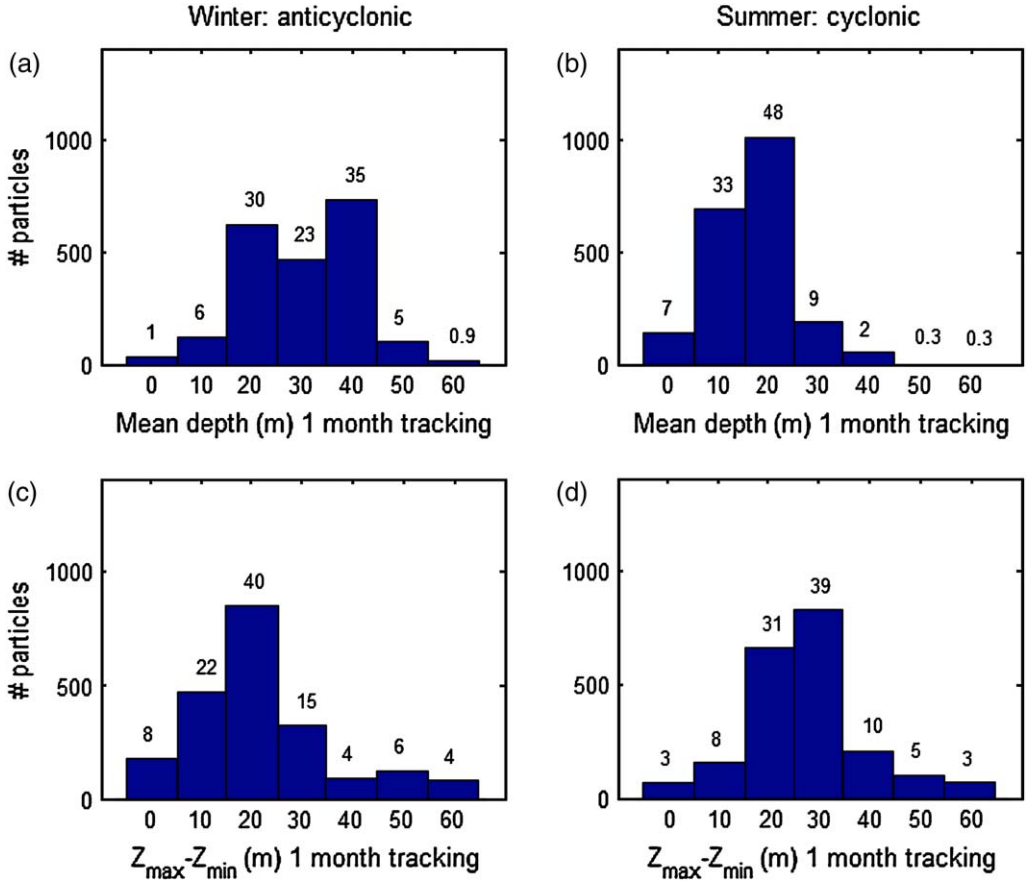

Fig. 5. Histograms of the mean depth (m) in one-month tracking of the 3D trajectories for the (a) anticyclonic and (b) cyclonic gyre periods. Histograms of the maximum vertical excursion, for the 3D case, for the (c) anticyclonic and (d) cyclonic gyre periods. The figures in top of each bar are the % of particles for each depth range. The total number of particles is 2097.

the time period of less than a month, which is about the time from spawning to postlarve stage (2–3 weeks), can be as large as 40 km; this could mean that the postlarvae would reach or not a nursery area.

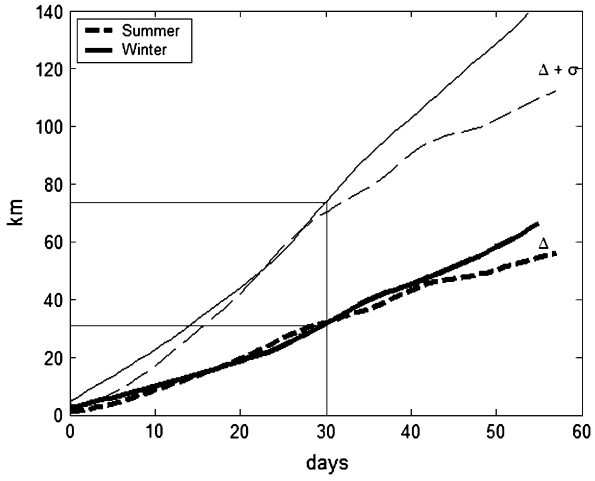

Fig. 6. Horizontal position difference between the 2D and the 3D trajectories for the anticyclonic (winter) and cyclonic (summer) gyre periods, respectively, as a function of time (days). Thick lines correspond to the mean and thin lines to the mean + one standard deviation. The total number of particles is 2097.

Acknowledgements

This research was financed by the Consejo Nacional de Ciencia y Tecnología (CONACyT) through grant 44055 and by the block funding of the Centro de Investigación Científica y de Educación Superior de Ensenada (CICESE). I thank Miguel Lavín, Oscar Velasco, Antoine Badan, and Manuel Figueroa for critically reading the manuscript.

References

Aragón-Noriega, E.A., Calderón-Aguilera, L.E., 2001. Age and growth of shrimp postlarvae in the Upper Gulf of California. Aquatic Journal of Ichthyology and Aquatic Biology 4 (3), 99–104.

Backhaus, J.O., 1985. A three-dimensional model for the simulation of shelf sea dynamics. Deutsche Hydrographische Zeitschrift 38, 165–187.

Beier, E., 1997. A numerical investigation of the annual variability in the Gulf of California. Journal of Physical Oceanography 27, 615–632.

Beier, E., Ripa, P., 1999. Seasonal gyres in the northern Gulf of California. Journal of Physical Oceanography 29, 302–311.

Calderón-Aguilera, L.E., Marinone, S.G., Aragón-Noriega, E.A., 2003. Influence of oceanographic processes on the early life stages of the blue shrimp (*Litopeneaus stylirostris*) in the Upper Gulf of California. Journal of Marine Systems 924, 1–12.

Carbajal, N., 1993. Modeling of the circulation in the Gulf of California. Ph.D. thesis, Institute fur Meereskunde, Hamburg, 186 pp.

Carrillo-Bribiezca, L.E., Lavín, M.F., Palacios-Hernández, E., 2002. Seasonal evolution of the geostrophic circulation in the northern Gulf of California. Estuarine, Coastal and Shelf Science 54, 157–173.

Gutiérrez, O.Q., Marinone, S.G., Parés-Sierra, A., 2004. Lagrangian surface circulation in the Gulf of California from a 3D numerical model. Deep-Sea Research II 51 (6–9), 659–672.

Kochergin, V.P., 1987. Three-dimensional prognostic models. In: Heaps, N.S. (Ed.), Three-Dimensional Coastal Ocean Models. American Geophysical Union, Washington, DC.

Lavín, M.F., Durazo, R., Palacios, E., Argote, M.L., Carrillo, L., 1997. Lagrangian observations of the circulation in the northern Gulf of California. Journal of Physical Oceanography 27, 2298–2305.

Marinone, S.G., 2003. A three dimensional model of the mean and seasonal circulation of the Gulf of California. Journal of Geophysical Research 108 (C10), 3325. doi:10.1029/2002JC001720.

Marinone, S.G., Gutiérrez, O.Q., Parés-Sierra, A., 2004. Numerical simulation of larval shrimp dispersion in the northern region of the Gulf of California. Estuarine, Coastal and Shelf Science 60 (4), 611–617.

Palacios-Hernández, E., Beier, E., Lavín, M.F., Ripa, P., 2002. The effect of the seasonal variation of stratification on the circulation on the northern Gulf of California. Journal of Physical Oceanography 32, 705–728.

Proehl, J.A., Lynch, D.R., McGillicuddy, D.J., Ledwell, J.R., 2005. Modeling turbulent dispersion on the North Flank of Georges Bank using Lagrangian particle methods. Continental Shelf Research 25, 875–900.

Ross, O.N., Sharples, J., 2004. Recipe for 1-D Lagrangian particle tracking models in space-varying diffusivity. Limnology and Oceanography: Methods 2, 289–302.

Thorpe, S.E., Heywood, K.J., Stevens, D.P., Brandon, M.A., 2004. Tracking passive drifters in a high resolution ocean model: implications for interannual variability of larval krill transport to South Georgia, 204. Deep-Sea Research 51, 909–920.

Velasco-Fuentes, O.U., Marinone, S.G., 1999. A numerical study of the Lagrangian circulation in the Gulf of California. Journal of Marine Systems 22, 1–12.

Visser, A.W., 1997. Using random walk models to simulate the vertical distribution of particles in a turbulent water column. Marine Ecology Progress Series 158, 275–281.

Yao, T., Pond, S., Mysak, L.A., 1982. Low-frequency subsurface current and density fluctuations in the Strait of Georgia. Atmosphere Ocean 20, 340–356.